

A Hierarchical Approach to Dimensionality Reduction and Nonparametric Problems in the Polynomial Chaos Simulation of Transmission Lines

*Original*

A Hierarchical Approach to Dimensionality Reduction and Nonparametric Problems in the Polynomial Chaos Simulation of Transmission Lines / Manfredi, Paolo. - In: IEEE TRANSACTIONS ON ELECTROMAGNETIC COMPATIBILITY. - ISSN 0018-9375. - STAMPA. - 62:3(2020), pp. 736-745. [10.1109/TEMC.2019.2918724]

*Availability:*

This version is available at: 11583/2782214 since: 2022-04-13T09:31:34Z

*Publisher:*

IEEE

*Published*

DOI:10.1109/TEMC.2019.2918724

*Terms of use:*

This article is made available under terms and conditions as specified in the corresponding bibliographic description in the repository

*Publisher copyright*

IEEE postprint/Author's Accepted Manuscript

©2020 IEEE. Personal use of this material is permitted. Permission from IEEE must be obtained for all other uses, in any current or future media, including reprinting/republishing this material for advertising or promotional purposes, creating new collecting works, for resale or lists, or reuse of any copyrighted component of this work in other works.

(Article begins on next page)

# A Hierarchical Approach to Dimensionality Reduction and Nonparametric Problems in the Polynomial Chaos Simulation of Transmission Lines

Paolo Manfredi, *Senior Member, IEEE*.

**Abstract**—Polynomial chaos-based techniques recently became popular alternatives for the stochastic analysis of electrical circuits, especially in the context of signal integrity and electromagnetic compatibility investigations. Among the challenging issues of polynomial chaos, there are two longstanding limitations: curse of dimensionality (i.e., efficiency decrease as the number of random parameters is increased) and the inability to handle nonparametric variations (i.e., random variables that cannot be unambiguously parametrized upfront). This paper aims at covering this gap by putting forward a suitable hierarchical approach, with specific emphasis on transmission-line analysis. First, the problem is characterized by estimating the distribution of the transmission line per-unit-length parameters. Second, the obtained distribution is fitted using a multivariate mixture of Gaussians. The mixture of Gaussians is a flexible model that is capable of taking into account the existing dependence between inductance and capacitance entries in multiconductor lines. Next, appropriate orthogonal basis functions are generated based on a recent framework for non-Gaussian correlated random variables. Finally, the technique is combined with a stochastic Galerkin method to generate a deterministic and SPICE-compatible model that can be simulated in time domain. The proposed approach enables both dimensionality (hence, model order) reduction and handling of nonparametric variations. Application examples concerning cables with random cross-section illustrate and validate the methodology.

**Index Terms**—Cables, non-Gaussian correlation, polynomial chaos, signal integrity, stochastic Galerkin method, transmission lines, variability analysis, uncertainty quantification.

## I. INTRODUCTION

POLYNOMIAL CHAOS (PC) [1] has emerged in recent years as a robust approach for the uncertainty quantification in many domains, including electrical and electronic engineering [2]. PC consists of representing stochastic responses as suitable expansions of orthogonal polynomials that depend on the random parameters and their distribution. Specifically, PC has been extensively applied to circuit and transmission line analysis for signal integrity (SI) and electromagnetic compatibility (EMC) characterizations [3]–[8]. Both intrusive and non-intrusive approaches are available for the determination of the PC expansion coefficients [7].

PC exhibits a substantial efficiency improvement when compared to the blind Monte Carlo (MC) method. However, one of its main disadvantages is the generally poor scalability w.r.t. the number of uncertain parameters (the so-called “curse of dimensionality”). Moreover, since the PC model seeks a

model with explicit dependence on the random parameters through the polynomial basis, a fundamental requirement of PC is the preliminary parametrization of random inputs in terms of a *finite* and unambiguously defined set of *independent* random variables (RVs) [9]. A relevant example in the context of SI/EMC investigations for which this parametrization is not possible is the case, illustrated in Fig. 1, of a random cable cross-section that is generated by sequentially placing wires in a 2D area, progressively filling the remaining available space. Unless overly restrictive assumptions are made on the wire coordinates to a-priori avoid overlap, the position of subsequent wires is dependent on the specific positions of previously placed wires, and therefore it cannot be unambiguously parametrized upfront. In the past, the modeling of cable bundles with random wire placement received a wide attention from the EMC community. Popular empirical approaches to deal with this situation are to make restrictive assumptions on the wire separation, e.g., [10], [11], or to apply random wire permutations to a fixed cross-section [12]–[15].

Over the years, several techniques were proposed to alleviate the dimensionality issue. The approach in [16] allows approximating a large set of correlated parameters in terms of a reduced set of independent parameters, but it is valid only when the covariance matrix is of Gaussian type. Tensor-based approaches [17] work well for scalar outputs, but they become cumbersome for the modeling of an entire response (e.g., in frequency or time domain). In [18], [19], a hierarchical approach was proposed, where selected mid-level parameters that individually depend on many low-level uncertain parameters were represented each by a single synthetic uncertain parameter, with corresponding (non-standard) distribution. To this end, special basis functions were constructed that were orthogonal based on the various distributions of the mid-level parameters, and used to model high-level parameters (outputs) in a hierarchical fashion, as depicted in Fig. 2. Nevertheless,

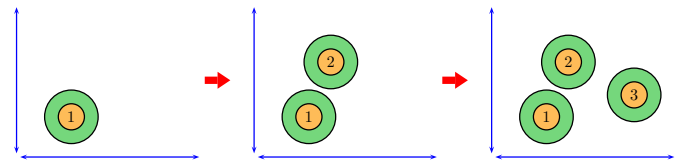


Fig. 1. Sequential generation of a random cable cross-section. The position of wire #1 is parametrized by the random coordinates spanning the available area (indicated by the blue arrows). The position of wires #2 and #3 cannot be parametrized upfront instead, as it is affected by previously placed wires.

P. Manfredi is with the Department of Electronics and Telecommunications, Politecnico di Torino, Turin 10129, Italy (e-mail: paolo.manfredi@polito.it).

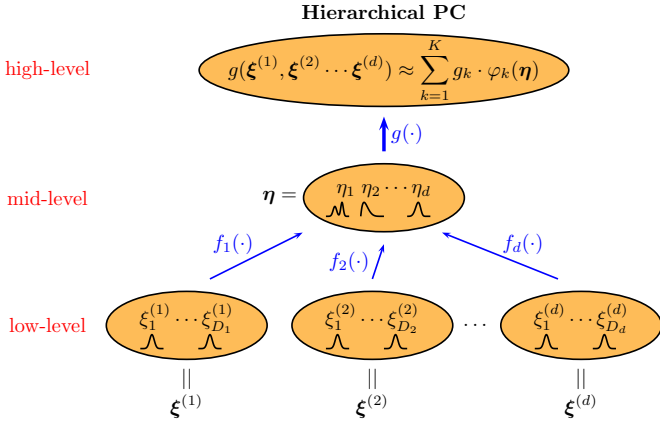


Fig. 2. Hierarchical PC: a set of mid-level variables  $\eta$ , are each an individual function  $f_i$  ( $i = 1, \dots, d$ ) of a set of low-level variables  $\xi^{(i)}$  (e.g., Gaussian distributed). A high-level output  $g$  that is function of the low-level variables through the mid-level ones, is expressed in terms of polynomials that are orthogonal based on the (non-standard) distribution of the mid-level variables.

this approach is only applicable as long as the mid-level parameters are mutually independent, i.e., they depend on different sets of low-level parameters, and no dependence exists between these sets.

In the framework of transmission-line analysis, random geometrical and material properties could be in principle regarded as low-level variables, per-unit-length (p.u.l.) parameters as mid-level variables, and line voltages and currents as high-level output variables. However, the approach in [18] is not applicable as is, since each matrix entry depends on the same set of physical parameters, and the above method would fail to track this dependence. Deliberately neglecting the existing dependence would unavoidably lead to erroneous and inconsistent results. As far as the handling of nonparametric variables is concerned, to the author's best knowledge no solution is available in the framework of PC. It should be noted that this limitation is common to both intrusive and non-intrusive PC implementations.

This paper puts forward a novel strategy that allows coping with both the above limitations simultaneously. The idea is similar to the hierarchical approach in [18]. Per-unit-length (p.u.l.) inductance and capacitance parameters are considered as mid-level variables that depend on low-level cross-sectional parameters (e.g., geometrical and material properties). As noted before, all the p.u.l. inductance and capacitance matrix entries are in principle related to each other, thus making the use of [18] impossible for the above purpose. To overcome the aforementioned difficulty, the p.u.l. inductance and capacitance matrix entries are simultaneously modeled as a unique set of *correlated* random parameters. For this purpose, a mixture of Gaussians (MoG) distribution is fitted to a given number of stochastic samples thereof. The MoG is a powerful and flexible model that can approximate correlated distributions of arbitrary shape. In this way, the dependency between matrix entries is tracked through correlation. Next, suitable orthogonal basis functions for the correlated MoG-variables are constructed using the recent approach in [20], which uses a Gram-Schmidt orthogonalization (GSO) and generically applies to

non-Gaussian correlated distributions. Finally, a stochastic Galerkin method (SGM) [9] is applied to build a deterministic and SPICE-compatible circuit model that can be simulated in time domain to obtain the coefficients of the PC model of the line voltages and currents [7]. Two application examples, concerning the analysis of wiring structures, illustrate and validate the advocated technique.

The remainder of the paper is organized as follows. Section II briefly recalls the main notions of the classical PC that are necessary for the subsequent developments. Section III defines the problem and discusses current limitations. Section IV outlines the proposed hierarchical framework. Illustrative applications example are discussed in Section V. Finally, conclusions are drawn in Section VI.

## II. POLYNOMIAL CHAOS OVERVIEW

This section briefly recalls the necessary notions about the classical PC for the stochastic analysis of multiconductor transmission lines with independent RVs. This subject is extensively covered in the available literature (e.g., [7]). The extension to non-Gaussian correlated RVs, as needed for the proposed hierarchical approach, is discussed in Section IV.

Assume a multiconductor transmission line with  $n$  signal conductors be affected by a set of  $D$  random parameters  $\xi = [\xi_1 \dots \xi_D]$  (typically, geometrical and/or material properties). The pertinent stochastic transmission-line equations in time domain read:

$$\begin{cases} \frac{\partial}{\partial z} \mathbf{v}(t, z, \xi) = -\mathbf{L}(\xi) \frac{\partial}{\partial t} \mathbf{i}(t, z, \xi) \\ \frac{\partial}{\partial z} \mathbf{i}(t, z, \xi) = -\mathbf{C}(\xi) \frac{\partial}{\partial t} \mathbf{v}(t, z, \xi), \end{cases} \quad (1)$$

where  $t$  and  $z$  denote time and longitudinal position, respectively. The  $n \times n$  p.u.l. inductance matrix  $\mathbf{L}$  and capacitance matrix  $\mathbf{C}$  depend on the cross-sectional properties, and hence also on the random parameters  $\xi$ . Vectors  $\mathbf{v} = (v_1, \dots, v_n)^T$  and  $\mathbf{i} = (i_1, \dots, i_n)^T$  collect the line voltages and currents, which are in turn stochastic as a result of the uncertainty in the transmission-line properties. Without loss of generality, conductor and dielectric losses are neglected in the following discussion. However, the proposed technique applies to lossy transmission lines without modification.

Any voltage and current, denoted generically with  $g$ , is expressed as a truncated PC expansion

$$g(\xi) \approx \hat{g}(\xi) = \sum_{k=1}^K g_k \varphi_k(\xi), \quad (2)$$

where the dependence on  $t$  and  $z$  has been omitted for brevity of notation. The functions  $\{\varphi_k\}_{k=1}^\infty$  form a complete basis of orthonormal polynomials based on the inner product

$$\langle f, g \rangle = \int_{\mathbb{R}^D} f(\xi) g(\xi) \rho(\xi) d\xi, \quad (3)$$

with the weighting function  $\rho(\xi)$  denoting the joint probability density function (PDF) of the RVs  $\xi$ . For the univariate case (i.e.,  $D = 1$  and scalar  $\xi$ ) and some standard distributions  $\rho(\xi)$ , orthogonal polynomials are already available [1]. For example, Hermite, Legendre, and Jacobi polynomials are orthogonal

when the weighting function  $\rho(\xi)$  in (3) is the Gaussian, uniform, or beta distribution, respectively. Orthonormality is often useful and readily achieved by proper normalization [21].

For multiple *independent* RVs, suitable multivariate polynomials are built as tensor-product combination of univariate polynomials in each variable:

$$\varphi_k(\xi) = \prod_{j=1}^D \varphi_{k_j}^{(j)}(\xi_j), \quad (4)$$

where  $\varphi_{k_j}^{(j)}(\xi_j)$  is a polynomial of degree  $k_j$  that is orthogonal w.r.t. the distribution of  $\xi_j$ . In the l.h.s. of (4),  $k$  is the scalar index identifying a vectorial multi-index element  $\mathbf{k} = [k_1, \dots, k_D] \in \mathcal{K}$ . Typically, the expansion is truncated to retain only polynomials up to a given *total degree*  $P$ , meaning that the set of multi-indices is defined as

$$\mathcal{K} = \{\mathbf{k} : \|\mathbf{k}\|_1 \leq P\}. \quad (5)$$

In this case, the cardinality of  $\mathcal{K}$  (i.e., the number of basis functions) is  $K = (P+D)!/(P!D!)$ . For practical applications in the SI/EMC context, second-order expansions ( $P = 2$ ) in conjunction with the SGM typically provide satisfactory accuracy [6]. The basis functions  $\{\varphi_k\}_{k=1}^K$  are further assumed to be sorted according to the graded lexicographic ordering (GLO). The case of *dependent* RVs is much less trivial instead, and subject of ongoing research [20], [22].

With the above definitions, if  $g(\xi)$  is a square-integrable function (i.e., it has finite variance), then the approximation  $\hat{g}$  of  $g$  converges exponentially in  $L^2$ -sense as the number of basis functions  $K$  is increased, i.e.,

$$\lim_{K \rightarrow \infty} \|g - \hat{g}\|_{L^2} = 0, \quad (6)$$

where the norm is based on the inner product (3).

Moreover, thanks to orthogonality, the first two statistical moments of  $\hat{g}$  (an estimate of the actual mean and variance of  $g$ ) are readily computed as

$$\mathbb{E}\{\hat{g}(\xi)\} = \int_{\mathbb{R}^D} \hat{g}(\xi) \rho(\xi) d\xi \equiv \langle \hat{g}, 1 \rangle = g_1 \quad (7)$$

and

$$\text{Var}\{\hat{g}(\xi)\} = \int_{\mathbb{R}^D} (\hat{g}(\xi) - \mathbb{E}\{\hat{g}(\xi)\})^2 \rho(\xi) d\xi = \sum_{k=2}^K g_k^2, \quad (8)$$

respectively.

Several techniques are available for the determination of the PC expansion coefficients  $g_k$ . Spectral approaches compute the coefficients by projection:

$$g_k = \langle g, \varphi_k \rangle = \int_{\mathbb{R}^d} g(\xi) \varphi_k(\xi) \rho(\xi) d\xi. \quad (9)$$

In particular, pseudo-spectral methods approximate the projection integral (9) by means of a multi-dimensional quadrature. The SGM builds an augmented, deterministic and fully coupled system of equations in all the unknown coefficients [3]:

$$\begin{cases} \frac{\partial}{\partial z} \tilde{\mathbf{v}}(t, z) &= -\tilde{\mathbf{L}} \frac{\partial}{\partial t} \tilde{\mathbf{i}}(t, z) \\ \frac{\partial}{\partial z} \tilde{\mathbf{i}}(t, z) &= -\tilde{\mathbf{C}} \frac{\partial}{\partial t} \tilde{\mathbf{v}}(t, z), \end{cases} \quad (10)$$

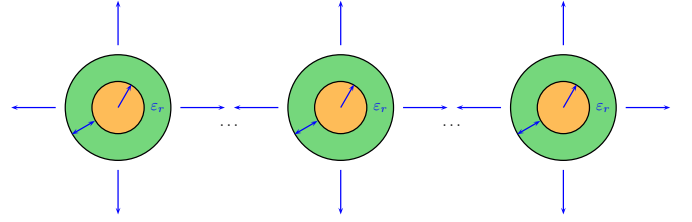


Fig. 3. Cable cross-section. The following geometrical and material parameters (indicated in blue) are assumed as RVs: conductor radius, dielectric thickness and relative permittivity, wire horizontal and vertical displacement.

where  $\tilde{\mathbf{v}}$  and  $\tilde{\mathbf{i}}$  collect the PC coefficients of all voltages and currents, respectively, and the  $Kn \times Kn$  p.u.l. matrices  $\tilde{\mathbf{L}}$  and  $\tilde{\mathbf{C}}$  are constructed based on the inductance and capacitance PC expansion coefficients, as discussed in Section IV-C. Other strategies fit the expansion (2) in a least-square sense [4] or by interpolation [5], [16], [23].

### III. PROBLEM DEFINITION

In order to properly motivate the proposed hierarchical framework, this section introduces two relevant examples in transmission-line analysis that have difficult or no solution in the state-of-the-art PC framework.

#### A. Hierarchical Problem with Dependent Random Parameters

Consider a cable with the cross-section depicted in Fig. 3. All the geometrical and material properties are considered to be independent RVs. Namely, for each wire:

- its radius;
- the thickness of its dielectric coating;
- the permittivity of its dielectric coating;
- its vertical displacement;
- its horizontal displacement.

All these uncertain parameters are indicated in blue in Fig. 3. For the sake of simplicity, the maximum horizontal displacement is suitably constrained to guarantee that overlap is avoided for any realization of the RVs. This is of course an overly restrictive assumption, but it is necessary to ensure each RV can be parametrized upfront. The case of nonparametric variations is discussed in the next section.

In the above scenario, a cable with  $N$  wires has  $D = 5N$  RVs in total. The p.u.l. inductance matrix  $\mathbf{L}$  and capacitance matrix  $\mathbf{C}$  depend on the above parameters [24], [25]. If one of the wires is taken as the reference conductor, the resulting matrices are of size  $n \times n$ , with  $n = N - 1$  being the number of signal wires. These matrices are symmetric by virtue of reciprocity. Therefore, the number of distinct RVs is  $n(n + 1)/2$  for each of the two matrices, leading to a total number of  $d = n(n + 1)$  parameters.

By analogy with the hierarchical strategy of Fig. 2, the  $D$  geometrical and material parameters are regarded as low-level variables, and the  $d$  p.u.l. inductance and capacitance matrix entries as mid-level variables, as illustrated in Fig. 4. Assuming that the first and second half of the  $\eta$ -variables correspond to

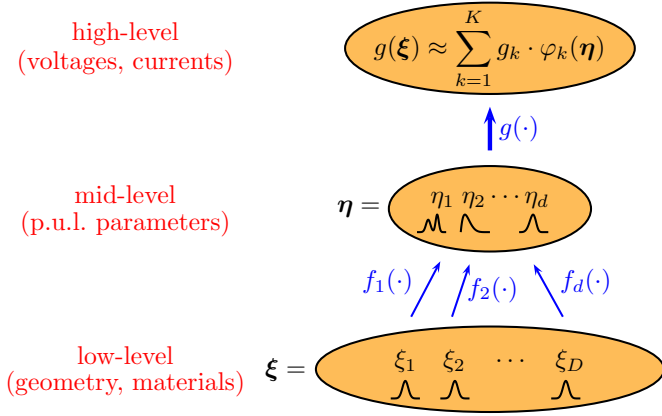


Fig. 4. Proposed hierarchical framework: the mid-level p.u.l. parameters  $\eta$  depend on a larger set of low-level random cross-sectional parameters  $\xi$ . High-level outputs (line voltages and currents) are modeled w.r.t. the smaller set of mid-level RVs through suitable polynomials.

the entries of the triangular part of  $\mathbf{L}$  and  $\mathbf{C}$ , respectively, leads to the following definition of the mid-level variables:

$$\begin{aligned} \mathbf{L} &= \begin{pmatrix} L_{11} & L_{12} & \cdots & L_{1n} \\ L_{21} & L_{22} & \cdots & L_2 \\ \vdots & & \ddots & \vdots \\ L_{n1} & L_{n2} & \cdots & L_{nn} \end{pmatrix} = \begin{pmatrix} \eta_1 & \eta_2 & \cdots & \eta_n \\ \eta_2 & \eta_{n+1} & \cdots & \eta_{2n-1} \\ \vdots & & \ddots & \vdots \\ \eta_n & \eta_{2n-1} & \cdots & \eta_{\frac{d}{2}} \end{pmatrix} \\ \mathbf{C} &= \begin{pmatrix} C_{11} & C_{12} & \cdots & C_{1n} \\ C_{21} & C_{22} & \cdots & C_2 \\ \vdots & & \ddots & \vdots \\ C_{n1} & C_{n2} & \cdots & C_{nn} \end{pmatrix} = \begin{pmatrix} \eta_{\frac{d}{2}+1} & \eta_{\frac{d}{2}+2} & \cdots & \eta_{\frac{d}{2}+n} \\ \eta_{\frac{d}{2}+2} & \eta_{\frac{d}{2}+n+1} & \cdots & \eta_{\frac{d}{2}+2n-1} \\ \vdots & & \ddots & \vdots \\ \eta_{\frac{d}{2}+n} & \eta_{\frac{d}{2}+2n-1} & \cdots & \eta_d \end{pmatrix}. \end{aligned} \quad (11)$$

The main difference with the scenario of Fig. 2 is that the mid-level variables now depend on the *same* set of low-level ones, thereby violating the assumption of mutual independence. Therefore, despite the inherent hierarchy in the outlined scenario, the technique in [18] cannot be applied.

Table I indicates the number of low- and mid-level variables for the example of Fig. 3 and increasing wire number  $N$ . The corresponding number  $K$  of PC basis functions, as required to model such a number of RVs with a second-order PC expansion ( $P = 2$ ), is also indicated. Clearly, as long as  $d < D$ , i.e., for a moderate number of conductors  $N$ , a substantial dimensionality compression can be achieved by expanding high-level variables w.r.t. to the mid-level RVs rather than the low-level RVs. The compression is even larger if higher order expansions are considered.

It is important to note that, because of the hierarchical dependence, high-level variables are typically a smoother function of the mid-level variables than of the low-level variables, thus implying that, with the proposed technique, an accurate expansion could be obtained with a lower order  $P$ . A similar approach is in general applicable whenever the number of p.u.l. matrix entries is smaller than the number of geometrical and material parameters.

TABLE I  
NUMBER OF LOW- AND MID-LEVEL PARAMETERS, AND CORRESPONDING SECOND-ORDER PC EXPANSION TERMS, FOR THE SCENARIO OF FIG. 2.

	low-level		mid-level	
wires	parameters	expansion terms	parameters	expansion terms
$N$	$D = 5N$	$K = \frac{(P+D)!}{P!D!}$	$d = N(N-1)$	$K = \frac{(P+d)!}{P!d!}$
2	10	66	2	6
3	15	136	6	28
4	20	231	12	91
5	25	351	20	231

### B. Nonparametric Variations: Randomized Cross-Section

In order to relax the constraint on the horizontal displacement of the wires, leading to a more realistic scenario while still avoiding overlaps, a sequential approach has to be implemented. Wires are placed one after another, instead of drawing their positions simultaneously as a single realization.

In particular, the strategy illustrated in Fig. 5 is adopted in this paper. A given cross-sectional area, in which the wires are allowed to be located, is subdivided into a fine grid. The coordinates of the first wire are then drawn randomly (with uniform distribution) within the entire available area. Next, one of the grid elements (shown in azure in Fig. 5) is randomly selected to accommodate the center of the second wire. To avoid overlap, the grid elements containing points that are closer to the first wire than twice the wire radius are excluded from the candidates, resulting in the blank space around the first wire. Therefore, azure elements in Fig. 5 indicate allowed locations. Once an allowed grid element is randomly selected, the wire center is further drawn randomly within the area of that grid element. Briefly speaking, the grid subdivision allows enforcing the non-overlap condition over a discrete, rather than a continuous set of elements. The size of the grid elements determines the discretization of the boundary between overlap and non-overlap regions.

The procedure is iterated by properly excluding each time the area around the newly placed wires, thereby gradually reducing the number of available locations, as shown in Fig. 5b and Fig. 5c. It should be noted that the proposed approach is more efficient than randomly drawing all the wire positions as a single realization, and checking for possible overlaps a-posteriori, as this may lead to a large number of instances being rejected. With the proposed procedure instead, unavailable positions are discarded beforehand.

In this second scenario, the wire coordinates cannot be explicitly expressed as a RV, and therefore the set of low-level parameters  $\xi$  is not even identifiable! This in turn implies that no state-of-the-art PC-based technique is applicable, and an MC analysis was so far the only viable solution for variability analysis.

## IV. PROPOSED HIERARCHICAL STRATEGY

In this section, a new hierarchical strategy is put forward, which aims at expressing the problem in terms of the mid-level



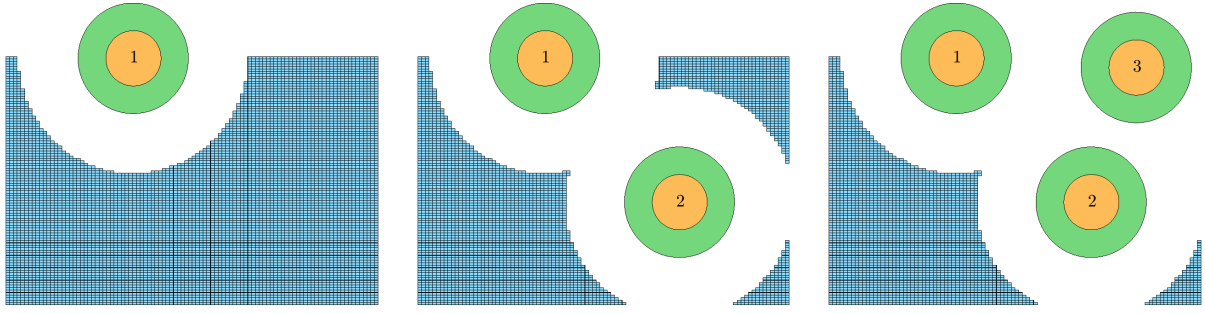


Fig. 5. Illustration of the proposed nonparametric wire positioning strategy. Wire #1 is randomly placed within the initial available area (left panel). Azure rectangles indicate the remaining allowed grid elements after placing the first wire. The center of wire #2 is randomly placed in one of the azure grid elements, causing more grid elements to become unavailable (central panel). The procedure is repeated for wire #3 (right panel).

variables  $\boldsymbol{\eta}$  (p.u.l. inductance and capacitance matrix entries) in place of the low-level variables  $\boldsymbol{\xi}$  (geometrical and material parameters, when explicitly available). As already pointed out, when the number of mid-level variables  $d$  is smaller than the number of low-level variables  $D$ , the PC model complexity is substantially reduced. Moreover, the hierarchical approach allows dealing with nonparametric problems, for which the low-level variables  $\boldsymbol{\xi}$  cannot be explicitly defined.

#### A. Mixture of Gaussians Fit

The starting point is the estimation of the distribution of the mid-level variables. To this end, a sufficiently large number of samples of the p.u.l. inductance and capacitance matrices is computed. This can be done in an MC fashion, after generating random instances of the cable cross-section (as described for example in Section III) and using the method in [24], [25]. For a parametric problem like the one of Section III-A, the PC-based technique in [26] can be alternatively used. It is important to remark that the calculation of samples of the inductance and capacitance matrices usually requires a negligible computational time when compared, e.g., to a transient analysis in SPICE.

Next, the distribution  $\rho(\boldsymbol{\eta})$  of the inductance and capacitance matrix entries is fitted using a MoG, i.e., a weighted sum of multivariate Gaussian components:

$$\begin{aligned} \rho(\boldsymbol{\eta}) &= \sum_{m=1}^M w_m \mathcal{N}(\boldsymbol{\eta} | \boldsymbol{\mu}_m, \boldsymbol{\Sigma}_m) \\ &= \sum_{m=1}^M \frac{w_m}{\sqrt{\det(2\pi\boldsymbol{\Sigma}_m)}} e^{-\frac{1}{2}(\boldsymbol{\eta}-\boldsymbol{\mu}_m)^T \boldsymbol{\Sigma}_m^{-1}(\boldsymbol{\eta}-\boldsymbol{\mu}_m)}, \end{aligned} \quad (12)$$

where the weights of each component satisfy

$$\begin{cases} w_m > 0 & \forall m \\ \sum_{m=1}^M w_m = 1 \end{cases}. \quad (13)$$

The function `fitgmdist`, available in MATLAB, is used for this purpose. The function provides weights  $w_m$ , means  $\boldsymbol{\mu}_m \in \mathbb{R}^d$ , and correlation matrices  $\boldsymbol{\Sigma}_m \in \mathbb{R}^{d \times d}$ , given the number of desired MoG components  $M$ .

#### B. Orthogonal Basis for the Mixture of Gaussian Distribution via Gram-Schmidt Orthogonalization

For joint distributions of dependent variables, like (12), suitable orthogonal basis functions needs to be computed. A recent approach based on GSO [20] is adopted for this purpose.

The starting point of the GSO is a set of linearly independent multivariate polynomials. The set of multivariate *monomials*  $\{\Psi_k(\boldsymbol{\eta}) = \eta_1^{k_1} \cdots \eta_d^{k_d}\}_{k=1}^K$  is used, with multi-indices  $\mathbf{k} \in \mathcal{K}$  defined as in (5), i.e., with total degree truncation and sorted in the GLO. The first basis function is simply taken to be  $\varphi_1(\boldsymbol{\eta}) = 1$ . The remaining basis functions  $\varphi_k$ , for  $k > 1$ , are recursively computed as

$$\begin{cases} \hat{\varphi}_k(\boldsymbol{\eta}) &= \Psi_k(\boldsymbol{\eta}) - \sum_{j=1}^{k-1} \mathbb{E}\{\Psi_k(\boldsymbol{\eta})\varphi_j(\boldsymbol{\eta})\}\varphi_j(\boldsymbol{\eta}) \\ \varphi_k(\boldsymbol{\eta}) &= \frac{\hat{\varphi}_k(\boldsymbol{\eta})}{\sqrt{\mathbb{E}\{\hat{\varphi}_k^2(\boldsymbol{\eta})\}}}. \end{cases} \quad (14)$$

The expectations in (14) are mere scalar coefficients. For small dimensions, they can be computed by numerically integrating (7). It should be noted that the weighting function in the integral is in this case the MoG distribution (12).<sup>1</sup> For higher dimensions, a tensor-train decomposition can be used, as suggested in [22]. A reasonable approximation, however, is obtained via MC integration. This is computationally tractable, since only closed-form functions need to be evaluated, namely the monomials  $\{\Psi_k(\boldsymbol{\eta})\}_{k=1}^K$ , the progressively generated basis functions  $\{\varphi_k(\boldsymbol{\eta})\}_{k=1}^K$ , and the MoG PDF (12).

#### C. Stochastic Galerkin Method

Once the basis functions are available, an SGM is used to calculate the expansion coefficients of the high-level variables, i.e., the voltages and currents at the line terminals. The approach involves the calculation of deterministic and  $K$ -times augmented p.u.l. inductance and capacitance matrices that define the equivalent transmission-line equation (10), whose voltage and current unknowns are the sought-for PC expansion coefficients of the actual voltages and currents.

<sup>1</sup>In MATLAB, a function for the evaluation of a MoG distribution is available as a method of the corresponding class.

The equivalent p.u.l. inductance and capacitance matrices in (10) are obtained as

$$\tilde{\mathbf{L}} = \sum_{k=1}^K \mathbf{A}_k \otimes \mathbf{L}_k, \quad \tilde{\mathbf{C}} = \sum_{k=1}^K \mathbf{A}_k \otimes \mathbf{C}_k, \quad (15)$$

where  $\otimes$  denotes the Kronecker product,  $\mathbf{A}_k \in \mathbb{R}^{K \times K}$  is a matrix with entries

$$[\mathbf{A}_k]_{ij} = \langle \varphi_k \varphi_j, \varphi_i \rangle, \quad (16)$$

whereas  $\mathbf{L}_k$  and  $\mathbf{C}_k$  are the PC expansion coefficients of the p.u.l. inductance and capacitance matrices computed w.r.t. the basis (14). Recalling that the RVs  $\boldsymbol{\eta}$  correspond to the p.u.l. matrix entries themselves, see (11), the coefficients are readily computed as the projection (9) of these variables:

$$[\mathbf{L}_k]_{ij} = \int_{\mathbb{R}^d} \eta_{\frac{d}{2} - (n-i+1)((n-i+1)+1)/2 + j - i + 1} \varphi_k(\boldsymbol{\eta}) \rho(\boldsymbol{\eta}) d\boldsymbol{\eta}$$

$$[\mathbf{C}_k]_{ij} = \int_{\mathbb{R}^d} \eta_{d - (n-i+1)((n-i+1)+1)/2 + j - i + 1} \varphi_k(\boldsymbol{\eta}) \rho(\boldsymbol{\eta}) d\boldsymbol{\eta}, \quad (17)$$

where the integral can be computed again by either numerical or MC integration. The augmented transmission line described by (10) is simulated in SPICE to obtain the transient PC expansion coefficients.

## V. APPLICATION EXAMPLES

In this section, the proposed hierarchical approach for dependent RVs is applied to the variability analysis of two cable lines.

### A. Two Wires with Random Geometric and Material Properties

This first application example considers the case of  $N = 2$  wires with random geometrical and material properties, as described in Section III-A. Specifically, their nominal values are as follows:

- wire radius  $r_w = 0.75$  mm;
- thickness of dielectric coating  $t_d = 0.4$  mm;
- relative permittivity of dielectric coating  $\varepsilon_r = 2.6$ ;
- distance between the wires  $d = 1$  cm.

The wire radius, as well as the thickness and permittivity of the dielectric coating, are assumed to be independent Gaussian RVs with a 10% relative standard deviation. The horizontal and vertical coordinates of each wire are ascribed a Gaussian distribution with a standard deviation of 1 mm. Although a Gaussian RVs can in principle take values infinitely away from the mean, overlap is extremely unlikely with the above parameters. The total number of RVs is  $D = 10$ .

One of the wires is taken as reference conductor, thus the corresponding transmission line is described by scalar p.u.l. inductance  $L$  and capacitance  $C$ . These are associated to mid-level variables  $\eta_1 = L$  and  $\eta_2 = C$ . Figure 6 visualizes their statistical distribution. In particular, Fig. 6(a) is a scatter plot of the computed inductance and capacitance samples, exhibiting nonlinear dependence. Indeed, there is an inverse relationship between the p.u.l. inductance and capacitance [25]. The marker color indicates the empirical probability of the corresponding

sample, with warmer colors denoting higher probability. Furthermore, Fig. 6(b) is a color plot of the MoG distribution with  $M = 8$  components that is fitted to the inductance and capacitance samples. The number of MoG components has been selected based on a convergence analysis of the difference between the empirical and fitted distribution, resulting in a good agreement between the two.

Next, orthogonal basis functions are built w.r.t. to the MoG distribution of these mid-level variables. By choosing order  $P = 2$ , and with  $d = 2$ , the starting set of (bivariate) monomials for the GSO is  $\{1, \eta_1, \eta_2, \eta_1^2, \eta_1\eta_2, \eta_2^2\}$ . Table II reports the six orthonormal polynomials resulting from the GSO, and the PC expansion coefficients of the p.u.l. inductance and capacitance. These are just the projection of the linear functions  $\eta_1$  and  $\eta_2$  onto the basis in Table II. Therefore, the coefficients of degree higher than one are zero.

A transient SPICE simulation is performed, in which the line is considered to be 20-cm long, fed with a voltage pulse source having an internal resistance of 100  $\Omega$ , and terminated by a capacitance of 1 pF, as illustrated in Fig. 7. The pulse source has an amplitude of 1 V, rise/fall times of 200 ps, and a duration of 2.8 ns at half amplitude. The output quantities of interest are the voltages at the near- and far-end terminations of the line, denoted as  $v_{NE}$  and  $v_{FE}$ , respectively.

To obtain reference results, an MC analysis is performed using the available 10000 samples of the p.u.l. inductance and capacitance. For the PC-based simulation instead, two scenarios are considered. The first one follows the rationale of the classical PC, in which the line voltages and currents (high-level variables) are expanded in terms of the actual (low-level) RVs, i.e., the 10 geometrical and material parameters. Hermite basis functions are adopted because of the Gaussian distribution of the underlying parameters, and the approach in [26] is used to calculate the pertinent PC expansion coefficients of the p.u.l. inductance and capacitance. In this case, higher-order coefficients are non-null owing to the nonlinear relationship between p.u.l. and uncertain parameters. In the second scenario, the line voltages and currents are expanded in terms of the two p.u.l. parameters (inductance and capacitance), using the new basis functions in Table II. In both cases, the augmented p.u.l. inductance and capacitance matrices are constructed via (15) and the Branin's method [27] is used to implement the corresponding equivalent lines in SPICE.

Figure 8 shows the results for the near-end terminal voltage. The solid gray lines in the top panel are a subset of 100 MC samples, giving a visual idea of the spread of the voltage due to the variability of the wire parameters. The solid blue line is the voltage mean obtained from the MC samples. The dashed red and dotted green lines are the means obtained with the classical and hierarchical PC implementations, respectively. The proposed hierarchical implementation is in very good agreement with the classical one. The high accuracy can be further appreciated from the bottom panel, which displays the voltage standard deviation with the same color code. A close-up on a time frame of high standard deviation shows that the new approach is even more accurate. This can be understood by the fact that the mid-level variables are represented exactly by the new basis functions, as opposed to the traditional im-

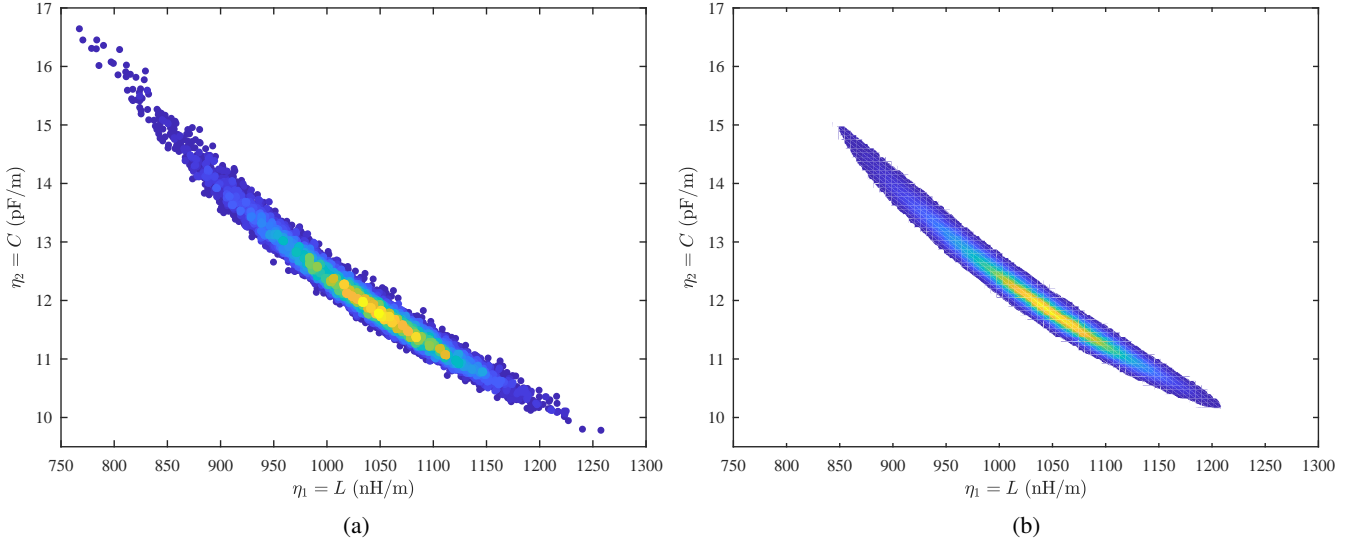


Fig. 6. Distribution of the p.u.l. inductance and capacitance for the two-wire example of Section V-A: (a) scatter plot of the computed samples, with marker colors indicating empirical probability (the warmer the color, the higher the probability); (b) color plot of the probability distribution of the MoG fit.

TABLE II  
ORTHONORMAL POLYNOMIALS FOR THE MID-LEVEL VARIABLES OF THE TWO-WIRE EXAMPLE OBTAINED FROM THE GSO, AND PC EXPANSIONS  
COEFFICIENTS FOR THE P.U.L. INDUCTANCE AND CAPACITANCE.

Basis functions	PCE coefficients	
	$L_k$ [nH/m]	$C_k$ [pF/m]
$\varphi_1(\eta_1, \eta_2) = 1$	1035.7	12.04
$\varphi_2(\eta_1, \eta_2) = 1.54 \cdot 10^{-2} \eta_1 - 15.93$	65.02	-0.846
$\varphi_3(\eta_1, \eta_2) = 7.84 \cdot 10^{-2} \eta_1 + 6.03 \eta_2 - 1.54 \cdot 10^2$	$\approx 0$	0.166
$\varphi_4(\eta_1, \eta_2) = 2.06 \cdot 10^{-4} \eta_1^2 - 4.84 \cdot 10^{-1} \eta_1 - 4.77 \eta_2 + 3.37 \cdot 10^2$	$\approx 0$	$\approx 0$
$\varphi_5(\eta_1, \eta_2) = 8.71 \cdot 10^{-4} \eta_1^2 + 6.47 \cdot 10^{-2} \eta_1 \eta_2 - 2.57 \eta_1 - 65.24 \eta_2 + 1.70 \cdot 10^3$	$\approx 0$	$\approx 0$
$\varphi_6(\eta_1, \eta_2) = 4.02 \cdot 10^{-3} \eta_1^2 + 5.88 \cdot 10^{-1} \eta_1 \eta_2 + 20.92 \eta_2^2 - 15.41 \eta_1 - 1.11 \cdot 10^3 \eta_2 + 1.47 \cdot 10^4$	$\approx 0$	$\approx 0$

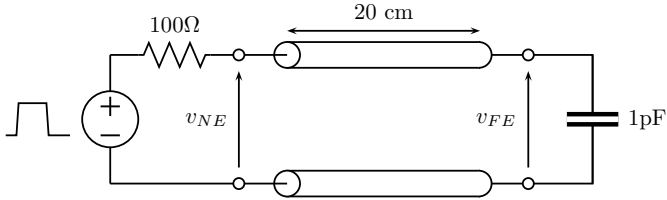


Fig. 7. Transmission line configuration for the application test case in Section V-A.

plementation, resulting in the PC expansion of the high-level variables being more accurate for a given order. Fig. 9 reports similar results for the far-end voltage, thus corroborating the above conclusions.

As far as the computational times are concerned, the MC analysis takes 3490 s, whereas the classical and hierarchical PC simulation take 357 s and 0.48 s, respectively. Therefore, the proposed approach achieves an impressive speed-up of  $740\times$  in transient simulation w.r.t. the traditional PC implementation, and of over  $7200\times$  w.r.t. MC. For the sake of completeness, the time required by the preliminary evaluation of the p.u.l. parameter samples is 48.9 s, whereas the calculation of the new basis functions for the hierarchical PC, based on

the numerical integration of the expectations in (14), takes 22.6 s. These onetime model-building steps are however not to be repeated when running simulations for different settings and/or loading conditions.

### B. Three Wires Above Ground with Randomized Cross-Section

The second example deals with a cable consisting of three wires, which lie above a perfect ground plane and are randomly placed according to the algorithm in Section III-B. The conductor radius is  $r_w = 7.5$  mil. The thickness of the dielectric coating is  $t_d = 10$  mil, and its relative permittivity is  $\epsilon_r = 3.5$ . The area in which the wires are allowed to be placed is a box of  $3 \times 2$  mm centered 3 cm above the ground plane. The cable configuration is illustrated in Fig. 10. The wires are 30-cm long and they are terminated by capacitances of 2 pF at the far end. At the near end, one of the wires is excited by a Gaussian-modulated sinusoidal voltage source with a frequency of 250 MHz, an amplitude of 1 V, a root-mean-square width of 10 ns, and an internal resistance of 50  $\Omega$ . The remaining wires are terminated by 50- $\Omega$  resistors.

A set of 10000 randomized cross-section instances are generated. The corresponding distribution of the  $d = 12$  entries of the triangular parts of the pertinent  $3 \times 3$  p.u.l.



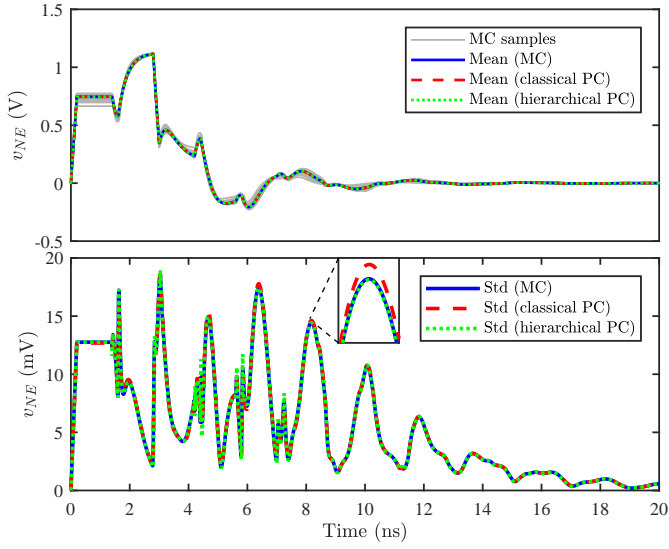


Fig. 8. Near-end voltage for the two-wire line. Top panel: MC samples and average voltage obtained from MC, classical PC and new hierarchical PC; bottom panel: standard deviation obtained with the same three approaches.

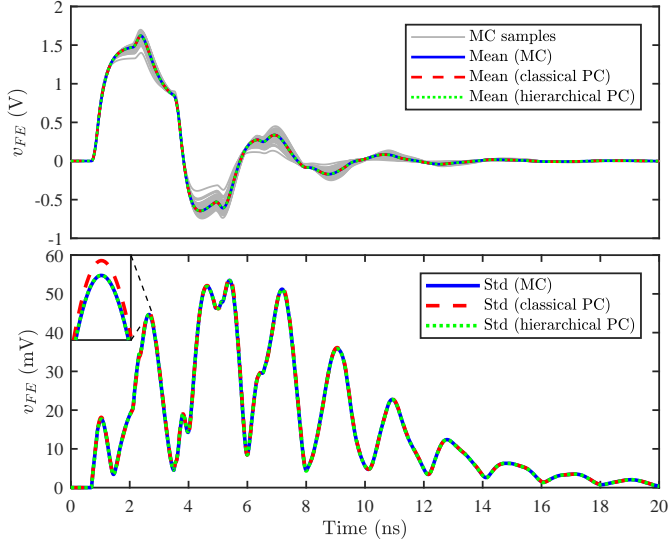


Fig. 9. Far-end voltage for the two-wire line. Curve identification is as in Fig. 8.

inductance and capacitance matrices is fitted using a MoG with  $M = 20$  components. Suitable orthonormal basis functions are constructed via the GSO. It should be noted that, given the nonparametric nature of the variation of the wire coordinates, the traditional PC framework cannot be applied to this example.

Figure 11 shows the spread and the corresponding mean (top panel) of the far-end crosstalk on one of the two victim wires, as well as its standard deviation (bottom panel). The statistical estimates are computed with both MC (solid blue line) and the proposed hierarchical PC with order  $P = 1$  (dotted green line). A very good agreement is obtained with just a first-order PC expansion. Similar results are obtained for the other victim wire and for the near-end crosstalk (results not shown here). The accuracy is further confirmed in Fig. 12 by a comparison

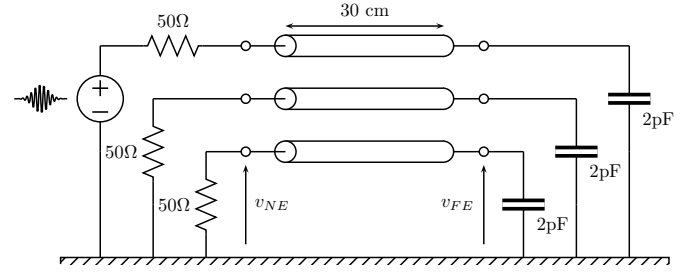


Fig. 10. Cable configuration for the application test case in Section V-B.

on the PDF of the far-end crosstalk, calculated at the time point of largest amplitude, i.e., about 31.1 ns, from both the MC samples (gray bars) and the PC expansion (green line).

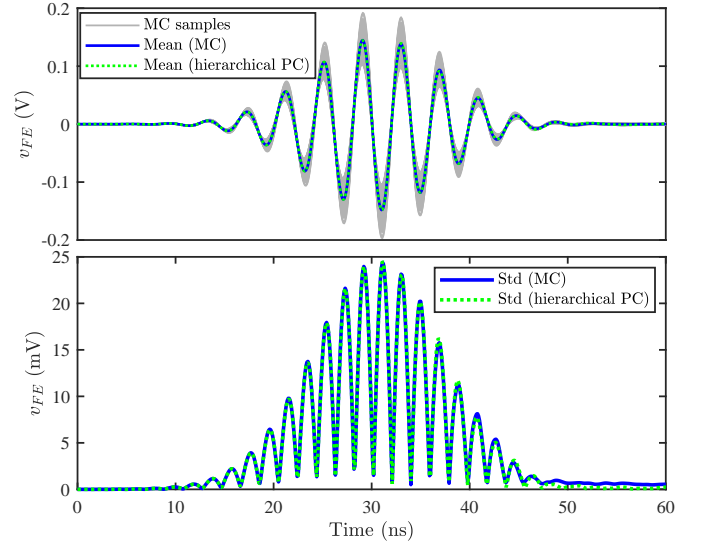


Fig. 11. Far-end crosstalk for the three wires above ground. Top panel: MC samples and average voltage obtained from MC and hierarchical PC; bottom panel: standard deviation obtained with the same two approaches.

As far as the computational times are concerned, the preliminary calculation of the samples of the p.u.l. inductance and capacitance matrices takes 226 s. The transient MC analysis based on these samples requires 4253 s. The proposed approach takes 4.8 s for the calculation of the basis functions, based on the MC integration of the expectations in (14), and 23 s for the transient SGM-based simulation. The proposed method achieves therefore a speed-up of over  $150\times$ .

## VI. CONCLUSIONS

This paper presented a hierarchical PC-based approach for the variability analysis of transmission lines. According to the proposed method, high-level stochastic output variables (line voltages and currents) are modeled as PC expansions of correlated mid-level variables (the p.u.l. parameters), rather than of low-level RVs (geometrical and material parameters). To this end, the distribution of the p.u.l. parameters is fitted using a MoG. Suitable orthonormal polynomials for the PC expansion are then computed via a GSO. Finally, an SGM is used to obtain transient results of the line voltages and currents in SPICE.

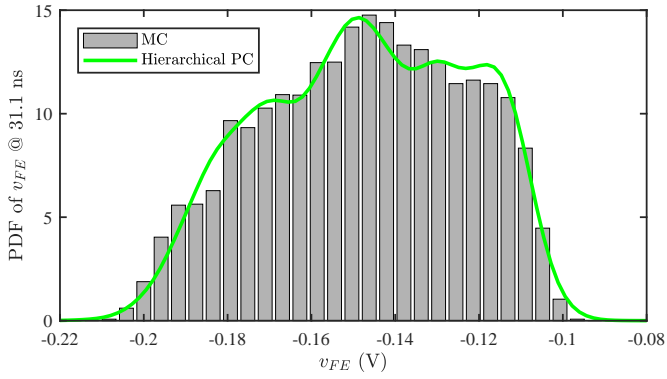


Fig. 12. PDF of the far-end crosstalk computed from the MC samples and hierarchical PC expansion.

This approach allows extending the applicability of PC-based variability analysis to scenarios in which the low-level variables cannot be unambiguously parameterized or defined, which was an unresolved limitation of any PC-based approach. Moreover, it enables a compression of the PC-problem size whenever the number of the mid-level variables is smaller than the number of low-level RVs, thus helping mitigate the “curse of dimensionality” issue. It is also noted that more accurate PC expansions can be obtained for a given order.

The benefits of the proposed technique were demonstrated by means of two application examples concerning wiring structures with random geometrical and/or material parameters. Further envisaged applications include transmission lines whose geometrical and/or material properties are described by continuous stochastic processes, like conductor surface roughness or inhomogeneous dielectrics with random local variations in the relative permittivity [28]. Continuous stochastic processes can be represented as a truncated expansion of a finite, yet large, number of random variables [29]. The uncertainty in these structures would therefore be described by a number of low-level RVs that is much larger than the number of mid-level p.u.l. parameters. Moreover, although here specifically conceived for transmission lines, it is expected that the advocated approach be applicable to problems with similar features in other engineering domains, including scenarios in which the distribution of the RVs is not assumed a priori, but rather estimated from measured data.

## REFERENCES

- [1] D. Xiu and G. E. Karniadakis, “The Wiener-Askey polynomial chaos for stochastic differential equations,” *SIAM J. Sci. Computation*, vol. 24, no. 2, pp. 619–622, 2002.
- [2] A. Kaintura, T. Dhaene, and D. Spina, “Review of polynomial chaos-based methods for uncertainty quantification in modern integrated circuits,” *Electronics*, vol. 7, no. 3, p. 30:1–21, Feb. 2018.
- [3] M. R. Rufuie, E. Gad, M. Nakhla, and R. Achar, “Generalized Hermite polynomial chaos for variability analysis of macromodels embedded in nonlinear circuits,” *IEEE Trans. Compon. Packag. Manuf. Technol.*, vol. 4, no. 4, pp. 673–684, Apr. 2014.
- [4] D. Spina, F. Ferranti, G. Antonini, T. Dhaene, and L. Knockaert, “Efficient variability analysis of electromagnetic systems via polynomial chaos and model order reduction,” *IEEE Trans. Compon., Packag., Manuf. Technol.*, vol. 4, no. 6, pp. 1038–1051, Jun. 2014.
- [5] M. Ahadi and S. Roy, “Sparse linear regression (SPLINER) approach for efficient multidimensional uncertainty quantification of high-speed circuits,” *IEEE Trans. Comput.-Aided Des. Integr. Circuits Syst.*, vol. 35, no. 10, pp. 1640–1652, Oct. 2016.
- [6] J. Bai, G. Zhang, D. Wang, A. P. Duffy, and L. Wang, “Performance comparison of the SGM and the SCM in EMC Simulation,” *IEEE Trans. Electromagn. Compat.*, vol. 58, no. 6, pp. 1739–1746, Dec. 2016.
- [7] P. Manfredi, D. Vande Ginste, I. S. Stievano, D. De Zutter, and F. G. Canavero, “Stochastic transmission line analysis via polynomial chaos methods: an overview,” *IEEE Electromagn. Compat. Mag.*, vol. 6, no. 3, pp. 77–84, 2017.
- [8] Ö. F. Yildiz, H. Brüns, and C. Schuster, “Variance-based iterative model order reduction of equivalent circuits for EMC Analysis,” *IEEE Trans. Electromagn. Compat.*, vol. 61, no. 1, pp. 128–139, Feb. 2019.
- [9] D. Xiu, “Fast numerical methods for stochastic computations: a review,” *Commun. Computational Physics*, vol. 5, no. 2–4, pp. 242–272, Feb. 2009.
- [10] S. Shiran, B. Reiser, and H. Cory, “A probabilistic model for the evaluation of coupling between transmission lines,” *IEEE Trans. Electromagn. Compat.*, vol. 35, no. 3, pp. 387–393, Aug. 1993.
- [11] D. Bellan, S. A. Pignari, and G. Spadacini, “Characterisation of crosstalk in terms of mean value and standard deviation,” *IEE Proc. Sci. Meas. Technol.*, vol. 150, no. 6, pp. 289–295, Nov. 2003.
- [12] A. Ciccolella and F. G. Canavero, “Stochastic prediction of wire coupling interference,” in *Proc. IEEE Int. Symp. Electromagn. Compat.*, Atlanta, GA, USA, Aug. 1995, pp. 5156.
- [13] S. Sun, G. Liu, J. L. Drewniak, and D. J. Pommerenke, “Hand-assembled cable bundle modeling for crosstalk and common-mode radiation prediction,” *IEEE Trans. Electromagn. Compat.*, vol. 49, no. 3, pp. 708–718, Aug. 2007.
- [14] M. Wu, D. G. Beetner, T. H. Hubing, H. Ke, and S. Sun, “Statistical prediction of “reasonable worst-case” crosstalk in cable bundles,” *IEEE Trans. Electromagn. Compat.*, vol. 51, no. 3, pp. 842–851, Aug. 2009.
- [15] D. Bellan and S. A. Pignari, “Efficient estimation of crosstalk statistics in random wire bundles with lacing cords,” *IEEE Trans. Electromagn. Compat.*, vol. 53, no. 1, pp. 209–218, Feb. 2011.
- [16] J. S. Ochoa and A. C. Cangellaris, “Random-space dimensionality reduction for expedient yield estimation of passive microwave structures,” *IEEE Trans. Microw. Theory Tech.*, vol. 61, no. 12, pp. 4313–4321, Dec. 2013.
- [17] Z. Zhang, T. Weng, and L. Daniel, “Big-data tensor recovery for high-dimensional uncertainty quantification of process variations,” *IEEE Trans. Compon. Packag. Manuf. Technol.*, vol. 7, no. 5, pp. 687–697, May 2017.
- [18] Z. Zhang, T. A. El-Moselhy, I. M. Elfadel, and L. Daniel, “Calculation of generalized polynomial-chaos basis functions and Gauss quadrature rules in hierarchical uncertainty quantification,” *IEEE Trans. Comput.-Aided Des. Integr. Circuits Syst.*, vol. 33, no. 5, pp. 728–740, May 2014.
- [19] Z. Zhang, X. Yang, I. V. Oseledets, G. E. Karniadakis, and L. Daniel, “Enabling high-dimensional hierarchical uncertainty quantification by ANOVA and tensor-train decomposition,” *IEEE Trans. Comput.-Aided Des. Integr. Circuits Syst.*, vol. 34, no. 1, pp. 63–76, Jan. 2015.
- [20] C. Cui and Z. Zhang, “Stochastic collocation with non-Gaussian correlated process variations: theory, algorithms and applications,” *IEEE Trans. Compon. Packag. Manuf. Technol.* (early access).
- [21] P. Manfredi, D. Vande Ginste, D. De Zutter, and F. G. Canavero, “Improved polynomial chaos discretization schemes to integrate interconnects into design environments,” *IEEE Microw. Wireless Compon. Lett.*, vol. 23, no. 3, pp. 116–118, Mar. 2013.
- [22] C. Cui and Z. Zhang, “Uncertainty quantification of electronic and photonic ICs with non-Gaussian correlated process variations,” [Online: <https://arxiv.org/abs/1807.01778>].
- [23] P. Manfredi, D. Vande Ginste, D. De Zutter, and F. G. Canavero, “Generalized decoupled polynomial chaos for nonlinear circuits with many random parameters,” *IEEE Microw. Wireless Compon. Lett.*, vol. 25, no. 8, pp. 505–507, Aug. 2015.
- [24] J. C. Clements, C. R. Paul, and A. T. Adams, “Computation of the capacitance matrix for systems of dielectric-coated cylindrical conductors,” *IEEE Trans. Electromagn. Compat.*, vol. 17, no. 4, pp. 238–248, Nov. 1975.
- [25] C. R. Paul and A. E. Feather, “Computation of the transmission line inductance and capacitance matrices from the generalized capacitance matrix,” *IEEE Trans. Electromagn. Compat.*, vol. 18, no. 4, pp. 175–183, Nov. 1976.
- [26] P. Manfredi and F. Canavero, “Efficient statistical extraction of the per-unit-length capacitance and inductance matrices of cables with random parameters,” *Advanced Electromagnetics*, vol. 4, no. 1, pp. 22–30, 2015.
- [27] C. R. Paul, *Analysis of Multiconductor Transmission Lines*, New York: Wiley, 1994.

- [28] A. Ajayi, P. Ingrej, P. Sewell, and C. Christopoulos, "Direct computation of statistical variations in electromagnetic problems," *IEEE Trans. Electromagn. Compat.*, vol. 50, no. 2, pp. 325–332, Nov. 1975.
- [29] M. Loève, *Probability Theory*, 4th ed. New York, NY, USA: Springer-Verlag, 1977.

PLACE  
PHOTO  
HERE

**Paolo Manfredi** (S'10–M'14–SM'18) received the M.Sc. degree in electronic engineering from the Politecnico di Torino, Torino, Italy, in 2009, and the Ph.D. degree in information and communication technology from the Scuola Interpolitecnica di Dottorato, Politecnico di Torino, in 2013.

From 2013 to 2014, he was a Postdoctoral Researcher with the EMC Group, Politecnico di Torino. From 2014 to 2017, he was a Postdoctoral Research Fellow of the Research Foundation–Flanders (FWO) with the Electromagnetics Group, Department of Information Technology, Ghent University, Ghent, Belgium. He is currently an Assistant Professor with the EMC Group, Department of Electronics and Telecommunications, Politecnico di Torino. His research interests comprise the several aspects of circuit and interconnect modeling and simulation, including statistical and worst-case analysis, signal integrity, and electromagnetic compatibility.

Prof. Manfredi was a recipient of an Outstanding Young Scientist Award at the 2018 Joint IEEE International Symposium on Electromagnetic Compatibility & Asia-Pacific Symposium on Electromagnetic Compatibility, the Best Paper Award at the 2016 IEEE Electrical Design of Advanced Packaging and Systems Symposium, the Best Oral Paper Award and the Best Student Paper Award at the 22nd and 19th IEEE Conference on Electrical Performance of Electronic Packaging and Systems, respectively, a Young Scientist Award at the XXX International Union of Radio Science General Assembly and Scientific Symposium, and an Honorable Mention at the 2011 IEEE Microwave Theory and Techniques Society International Microwave Symposium.